$u^*$ = local axial velocity within tube
$V$ = average velocity in downstream tube
$z^*$ = axial coordinate in cylindrical coordinate system

**Greek Letters**

$\alpha_1$ = constant of proportionality, defined in Equation (21)
$\Gamma$ = shear rate in steady laminar shearing flow
$\theta$ = tangential coordinate, Equation (1) only
$\theta_{fl}$ = relaxation time of fluid
$\mu$ = viscosity
$\rho$ = density
$\Theta$ = half-angle of conical region, Figure 10
$\tau$ = total stress tensor
$\tau_{11}, \tau_{22}, \tau_{33}$ = normal stress components of $\tau$
$(\tau_{11})_1, (\tau_{11})_3$, etc. = total stress components at control surfaces *1*, *3*, etc. respectively
$\tau_{12}$ = shear stress
$(\tau_{12})_w$ or $\tau_w$ = $\tau_{12}$ evaluated at the tube wall
$\tau'$ = stress deviator in Maxwell constitutive model
$II_d$ = second invariant of the deformation rate tensor d
$\varphi$ = adjustable parameter, to be determined experimentally

**LITERATURE CITED**


1. Astarita, G., *Ind. Eng. Chem. Fundamentals*, **6**, 257 (1967).
2. ———, and A. B. Metzner, *Atti Accad. Lincei*, **40**, VIII, 606 (1966).
3. Bagley, E. B., *Trans. Soc. Rheol.*, **5**, 355 (1961).
4. ———, A. M. Birks, and G. G. Warren, Film entitled "Polyethylene Flow Studies," Canadian Industries Ltd., McMasterville, Quebec (1961).
5. Ballman, R. L., *Rheologica Acta*, **4**, 137 (1965).
6. Bird, R. B., W. E. Stewart, and E. N. Lightfoot, "Transport Phenomena," John Wiley, New York (1960).
7. Boyce, R. J., W. H. Bauer, and E. A. Collins, *Trans. Soc. Rheol.*, **10**:2, 545 (1966).
8. Clegg, P. L., "The Rheology of Elastomers," p. 174, P. Mason and N. Wookey, eds., Pergamon Press, Nnew York (1958).
9. Collins, M., and W. R. Schowalter, *AIChE J.*, **9**, 804 (1963).
10. Cox, D., *Nature*, **193**, 670 (1962).
11. Drexler, L. H., M. Ch.E. thesis, Univ. Delaware, Newark, (1967).
12. Fabula, A. G., paper presented at fall meeting, Society of Rheology (1967).
13. Feig, J. E., M. Ch.E. thesis, Univ. Delaware, Newark, (1967).
14. Fields, T. R. and D. C. Bogue, *Trans. Soc. Rheology*, **12**, 39 (1968).
15. Hawkins, G. A., "Multilinear Analysis for Students in Engineering and Science," John Wiley, New York (1963).
16. Highgate, D., *Nature*, **211**, 1390 (1966).
17. Kaloni, P. N., *J. Phys. Soc., Japan*, **20**, 132 (1965).
18. *Ibid.*, **20**, 610 (1965).
19. King, R. G., *Rheol. Acta*, **5**, 35 (1966).
20. La Nieve, H. L., Ph.D. thesis, Univ. Tennessee, Knoxville (1966).
21. Marshall, R. J., and A. B. Metzner, *Ind. Eng. Chem. Fundamentals*, **6**, 393 (1967).
22. Metzner, A. B., *AIChE J.*, **13**, 316 (1967).
23. ———, J. L. White, and M. M. Denn, *Chem. Eng. Progr.*, **62**:12, 81 (1966).
24. ———, E. L. Carley, and I. K. Park, *Modern Plastics*, **37**, 133 (1960).
25. ———, W. T. Houghton, R. E. Hurd, and C. C. Wolfe., *Proc. Int. Symp. Second Order Effects Elasticity, Plasticity, Fluid Mech.*, 650 (1962).
26. Middleman, S., private correspondence (1967).
27. ———, and J. Gavis, *Phys. Fluids*, **4**, 963, 1450 (1961).
28. Oliver, D. R., *Can. J. Chem. Eng.*, **44**, 100 (1966).
29. Pearson, J. R. A., "Mechanical Principles of Polymer Melt Processing," Pergamon Press, New York (1966).
30. Philippoff, W., and F. H. Gaskins, *Trans. Soc. Rheol.*, **2**, 263 (1958).
31. Savins, J. G., *AIChE J.*, **11**, 673 (1965).
32. Schümmer, P., *Rheol. Acta*, **6**, 192 (1967).
33. Tordella, J. P., *Trans. Soc. Rheol.*, **1**, 203 (1957).
34. Uebler, E. A., Ph.D. thesis, Univ. Delaware, Newark (1966).
35. White, J. L., and A. B. Metzner, *Prog. Int. Research Thermophysical Transport Properties*, 748 (1962).
36. Wood, G. F., A. H. Nissan, and F. H. Garner, *J. Inst. Petrol.*, **33**, 71 (1947).


*Manuscript received November 6, 1967; revision received May 13, 1968; paper accepted May 15, 1968.*

# Temperature Profiles of Molten Flowing Polymers in a Heat Exchanger

**T. H. FORSYTH and N. F. MURPHY**

**Virginia Polytechnic Institute, Blacksburg, Virginia**

**The Graetz-Nusselt problem for polymeric flow in a constant wall temperature tube was studied, using a temperature-dependent power law rheological model and temperature dependent fluid properties. Theoretical results compare within 6% of experimental results. The fluid model predicts an experimentally observed temperature maxima at a reduced radius between 0.7 and 0.8 for cooling at low flow rates.**

Heat transfer to flowing polymer melts and solutions is a very important, but complex, operation in polymer processing. Some of the factors which complicate the analysis of nonisothermal polymeric flow are:

1. The viscosity of nearly all polymers is non-Newtonian and temperature dependent.
2. Polymer melts and many polymer solutions exhibit viscoelastic behavior.
3. The density of polymer melts is temperature and pressure dependent.
4. Viscous heating effects and cooling by expansion can be significant.
5. Thermal properties are temperature dependent.

The system being considered is the classical Graetz-Nusselt problem for heat transfer to a fluid which is flowing in a circular tube. The fluid enters the tube at a constant temperature, $T_1$, and with a flat velocity profile. The tube has a constant wall temperature, $T_w$.

Many analyses of this problem have been reported (*1* to *4*), most of which are more applicable to polymer solutions than to polymer melts. Several solutions can, however, be applied to polymer melts. Topper (*5*) considered the heat generation term a constant across the tube radius

T. H. Forsyth is with the Dow Chemical Company, Midland, Michigan.

for two cases, parabolic velocity profile and potential flow. Lyche and Bird (*6*) studied the flow of an incompressible power-law fluid without viscous heat generation, and Bird (*7*) extended the study to include viscous heat generation. Toor studied the effect of expansion combined with heat generation (*8*), and heat transfer to compressible fluids (*9, 10*). His results show that the inertial terms cannot be neglected for polymer melts.

Gee and Lyon (*11*) studied the cooling and isothermal flow of acrylic resins, by using a modified temperature-dependent Ellis rheological model. The fluid was assumed incompressible except for the cooling effect due to expansion. The steady state solution to the problem was obtained by Gauss-Seidel solution on a digital computer.

Four experimental measurements of temperature profiles of molten flowing polymers have been reported. Beyer and Dahl (*12*) studied heat transfer in an injection molder to determine the radial position $r/R$, at which a mass average temperature can be measured. Schott and Kaghan (*13*) studied temperature profiles in the die of an extruder. Griskey and Wiehe (*14*) studied temperature profiles of polyethylene and polypropylene during heating in a ⅜ in., schedule 80, pipe. Each of these three papers reports that the mass average temperature (average temperature with velocity as a weighting function) occurs at a radial position between 0.60 and 0.70. Griskey and Wiehe compared their experimental temperature profiles with the results of Lyche and Bird for negligible heat generation (*6*) and the results of Toor with significant heat generation (*8*), finding that viscous heating effects were not as significant as predicted by Toor. Recent experimental measurements of temperature profiles (*15*) for heating, cooling, and adiabatic flow of polyethylene, polystyrene, and polypropylene have shown that a maximum temperature occurs during cooling at low Graetz numbers, and that viscous heating effects were not as large as reported by Griskey and Wiehe.

This study was initiated to resolve the uncertainties which resulted from the investigation of Griskey and Wiehe on heat transfer to molten polymers. The object of the study reported here was to develop a solution to the continuity, momentum, and energy equations for a compressible, temperature-dependent fluid with power-law rheology, viscous heat generation, and variable properties, and to compare this solution to previous theories and experimental results.

## MATHEMATICAL MODEL

To approximate the physical system for flow of polymer melts in a circular tube, a compressible, power-law fluid with viscous heat generation and variable properties was assumed. Even though the real system is highly viscoelastic, a viscous rheological model was used. With viscoelastic rheological models, one could obtain a very general solution, but a direct comparison of results could not be made, since many of the constants are not valid for nonisothermal flow. Hence, we will neglect normal stresses, elastic strain energy, flow history, and time dependent effects, which can be important in many studies. For steady, laminar flow of a compressible fluid the continuity equation reduces to:

$$\frac{\partial(\rho V_z)}{\partial z} = 0 \tag{1}$$

For the continuity equation to be satisfied in the inlet region (where the velocity profile is changing from flat to parabolic) the radial velocity component must be nonzero. Equation (1) assumes that the radial and tangential velocity are small compared to the axial component.

Assuming negligible shear stress except in the axial direction by a radial velocity gradient, and a horizontal tube, the momentum equation is

$$\frac{\partial P}{\partial z} - \frac{1}{r}\frac{\partial}{\partial r}(r\,\tau_{rz}) = \rho\, V_z\left(\frac{\partial V_z}{\partial z}\right) \tag{2}$$

By further assuming that axial heat conduction is negligible compared to radial conduction, the energy equation for a compressible, purely viscous fluid with viscous heat generation is

$$\rho\, C_v V_z\left(\frac{\partial T}{\partial z}\right) = \frac{1}{r}\frac{\partial}{\partial r}\left(kr\frac{\partial T}{\partial r}\right) - T\left(\frac{\partial P}{\partial T}\right)_\rho\left(\frac{\partial V_z}{\partial z}\right) - \tau_{rz}\left(\frac{\partial V_z}{\partial z}\right) \tag{3}$$

Defining compressibility $\beta$ and coefficient of thermal expansion $\epsilon$ as

$$\beta = \frac{1}{\rho}\left(\frac{\partial \rho}{\partial P}\right)_T \tag{4}$$

$$\epsilon = \frac{-1}{\rho}\left(\frac{\partial \rho}{\partial T}\right)_P \tag{5}$$

The total derivative of density as a function of temperature and pressure is

$$d\rho = \left(\frac{\partial \rho}{\partial T}\right)_P dT + \left(\frac{\partial \rho}{\partial P}\right)_T dP \tag{6}$$

Substituting Equations (4) and (5) into (6) gives

$$d\ \ln\ \rho = -\epsilon dT + \beta dP \tag{7}$$

From Equation (7), at constant density:

$$\left(\frac{dP}{dT}\right)_\rho = \frac{\epsilon}{\beta} \tag{8}$$

It has been shown (*16*) that:

$$C_v + \frac{T\epsilon^2}{\rho\beta} = C_P \tag{9}$$

Combining Equations (3), (8), and (9), the energy equation becomes

$$\rho\, C_P V_z\left(\frac{\partial T}{\partial z}\right) = \frac{1}{r}\frac{\partial}{\partial r}\left(kr\frac{\partial T}{\partial r}\right) + T\epsilon V_z\frac{\partial P}{\partial z} - \tau_{rz}\left(\frac{\partial V_z}{\partial r}\right) \tag{10}$$

Over small intervals of temperature and pressure, Equation (7) can be integrated to obtain:

$$\rho = \rho_o\ \exp\ [\epsilon(T_o - T) + \beta(P - P_o)] \tag{11}$$

The rheological equation of state for the temperature-dependent power-law model is expressed as:

$$\tau_{rz} = -A\ \exp\ (-k_1 T)\left|\frac{dV_z}{dr}\right|^{n-1}\left(\frac{dV_z}{dr}\right) \tag{12}$$

Although the power-law index varies slightly with temperature, it can be assumed constant over 100°F. intervals (*17*).

To express the temperature and pressure dependence of $\beta$ and $\epsilon$, the Spencer-Gilmore (*18*) equation of state can be used in the following form:

$$1/\beta = (P + \pi)\left[1 + \frac{M_w b_o}{R_g T}(P + \pi)\right] \tag{13}$$

$$1/\epsilon = T + \frac{M_w b_o}{R_g}(P + \pi) \tag{14}$$

A linear function was used to express the temperature dependence of thermal conductivity and specific heat:

$$k = k_o [1 + b_1 (T - T_o)] \quad (15)$$

$$C_p = C_{po} [1 + c (T - T_o)] \quad (16)$$

## SOLUTION METHOD

The equations to be solved are the equations of change, Equations (1), (2), and (10); the temperature-dependent, power-law equation of state, Equation (12); and the temperature and pressure dependent properties, Equations (11) through (16). The boundary conditions for the system are:

$$\left.\begin{aligned} V_z &= 0 \\ T &= T_w \end{aligned}\right\} \quad r = R \quad \text{all } z \quad \text{(wall)}$$

$$\left.\begin{aligned} V_z &= \text{const} \\ T &= T_1 \end{aligned}\right\} \quad \text{all } r \quad z = 0 \quad \text{(inlet)}$$

$$\left.\begin{aligned} \frac{dV_z}{dr} &= 0 \\ \frac{dT}{dr} &= 0 \end{aligned}\right\} \quad r = 0 \quad \text{all } z \quad \text{(center)} \quad (17)$$

$$P = \Delta P \qquad z = 0$$

$$P = 0 \qquad z = L$$

To obtain a solution to this system of nonlinear, coupled, second-order, partial differential equations, numerical analysis was used. The differential equations were replaced by difference equations and solved by iteration. The two-dimensional grid scheme contained unequal intervals, with the smaller intervals in the inlet region of the tube.

The difference equations used were first-order and of the following type (*19*):

$$\frac{dZ}{dr} = \frac{Z(I) - Z(I-1)}{\Delta r} \quad (18)$$

Because Gauss-Seidel iteration requires that the initial estimate be very accurate, Gauss-Seidel iteration could not be used to obtain a general solution for this problem. Accordingly, a modified method of the following type was used:

$$Z_{p+1} = a\ Z_p + b\ Z'_{p+1} \quad (19)$$

Where $Z_p$ is the retained variable after $p$ iterations, $Z'_{p+1}$ is the calculated value after $p + 1$ iterations, and $a + b = 1$. When the index $a$ is greater than 0.5, convergence is slow but stability is improved.

The averaging of adjacent values was found to improve convergence, particularly for the first several iterations. The following correction was found to give a more stable, quicker converging solution:

$$Z(I) = a'\ Z(I) + b' \left[ \frac{Z(I+1) + Z(I-1)}{2.0} \right] \quad (20)$$

Where $Z(I)$ is the value of variable $Z$ at grid position $I$, and $a' + b' = 1$. The index $a'$ increases from zero toward one after each iteration is completed.

The boundary conditions, Equation (17), show that velocity and temperature are fixed at all the boundaries except the tube exit. To improve the results in the region of the tube exit, false (or nonphysical) boundaries (*19*) were used.

To summarize the solution method, the system of equations was approximated by difference equations, and solved by modified Gauss-Seidel interation, by using Equations (*19*) and (*20*) to improve stability and convergence. The data used (*15*) to obtain a solution is shown in Table 1.

Table 1. Polymer Property Values Used in Calculating Theoretical Temperature Profiles

| Symbol‡ | Polyethylene* | Polystyrene† |
|---|---|---|
| $\rho_o$ | 48.7 | 62.3 |
| $T_o$ | 300.0 | 300.0 |
| $P_o$ | 0.0 | 0.0 |
| $A\ 10^{-6}$ | 3.51 | 11.5 |
| $k_1\ 10^2$ | −1.22 | −1.27 |
| $n$ | 0.62 | 0.51 |
| $\pi$ | 6.85 | 3.9 |
| $b_o$ | 0.014 | 0.0132 |
| $C_{po}\ 10^4$ | 472.0 | 350.0 |
| $c$ | 1.0 | 18.0 |
| $k_o$ | 0.0284 | 0.0345 |
| $b_1$ | 0.0 | 0.567 |

* du Pont, Alathon 10
† Dow Styron 666 U
‡ units are shown in the Notation

## DISCUSSION

Table 2 shows a comparison of the experimentally observed flow rate and the flow rate predicted by the temperature dependent power-law rheological model. Although the results compare very well for polyethylene, the flow rates calculated for polystyrene are consistently higher than the observed flow rates. This may be due to the pressure dependence of viscosity of polystyrene (*20*) or to the higher elasticity of polystyrene melts. High elasticity would cause the pressure to be expended as recoverable elastic energy, rather than to increase the flow rate of the fluid. So for the range of flow rates studied, the mass flow rates are predicted very well for polyethylene, but poorly for polystyrene.

Table 2. Comparison of Predicted and Observed Flow Rates of Polyethylene and Polystyrene

| Material | $Gz$* | $T_w - T_1$ (°F.) | Predicted mass flow (g./min.) | Observed mass flow (g./min.) | % Difference† |
|---|---|---|---|---|---|
| polyethylene | 6.62 | 57 | 42.0 | 40.7 | − 3.1 |
| polyethylene | 3.79 | 0 | 23.4 | 23.3 | − 0.4 |
| polyethylene | 7.74 | −54 | 49.3 | 47.6 | − 3.5 |
| polystyrene | 3.63 | 35 | 45.8 | 34.2 | −25.4 |
| polystyrene | 2.33 | −18 | 32.4 | 22.0 | −32.1 |

* based on observed flow rate
† % difference $= \dfrac{\text{observed-predicted}}{\text{predicted}}$

The data (*15*) compared with the results of this study were reproducible to within 1°F., and measured temperatures are within about 3°F. of the true temperature, with the error due largely to heat conduction through the thermocouple, and bending of the thermocouple. To average out the errors, a large number of temperature profiles were measured. The experimental reduced temperatures ranged from 0.1 to 2.5.

A statistical comparison of the experimental and theoretical data at each radial position showed that the difference between theoretical and experimental reduced temperatures was 0.057 or less for 95% of the observations made. This correlation of reduced temperature profiles includes the polystyrene data, which showed large deviations between experimental and predicted flow rates. Hence, the method of predicting temperature profiles reported here is fairly accurate for most viscoelastic fluids, although the method for predicting flow rates may be seriously in error. The use of a viscoelastic rheological model might improve

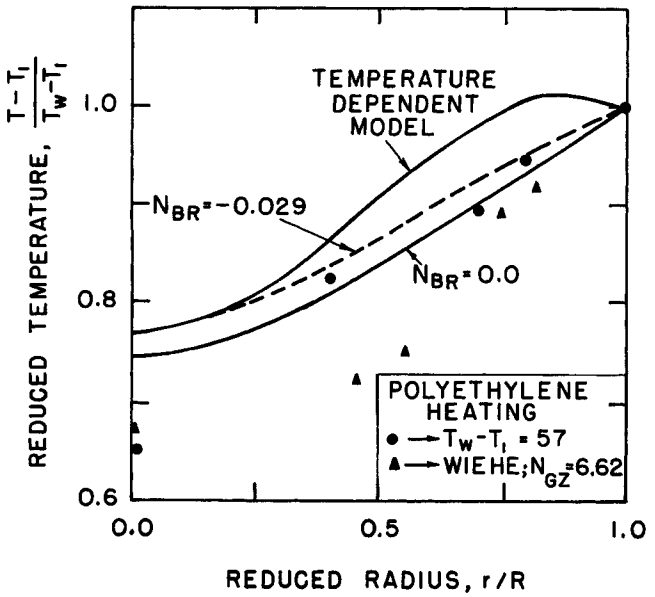


Fig. 1. Comparison of theoretical temperature profiles with experimental results for the heating of polyethylene.

the flow rate correlation, although it is not necessary for the temperature prediction.

Shown in Figure 1 is a comparison of the reduced temperature profiles for heating of polyethylene, as determined by (a) the Lyche-Bird model (an incompressible, constant property fluid without viscous heat generation), (b) Toor's model (a compressible, constant property fluid with viscous heat generation), (c) the model reported here (temperature-dependent power-law rheological model with variable properties), and (d) experimental data (*15*). Since the Brinkman number is a measure of the ratio of viscous heating to conductive heating, then the Brinkman number is zero for Bird's model and nonzero for Toor's model. The temperature-dependent power-law model reported here shows larger temperature changes than either of the constant property models. Even though the data shown in Figure 1 is best approximated by the constant property models, the data is within experimental accuracy of the temperature dependent model used in this study.

The results for nearly isothermal ($T_w \cong T_1$) flow of polyethylene are shown in Figure 2, indicating that the data more closely approximates the temperature-dependent model than either of the previous models.

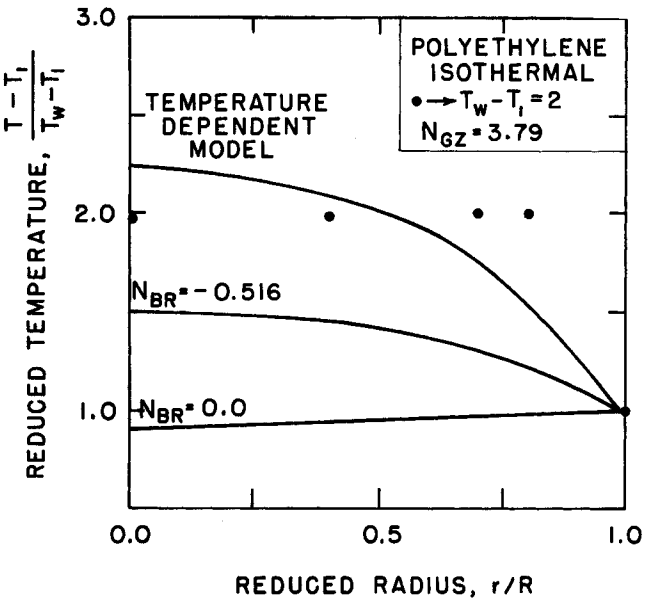


Fig. 2. Comparison of theoretical temperature profiles with experimental results for the isothermal flow of polyethylene.

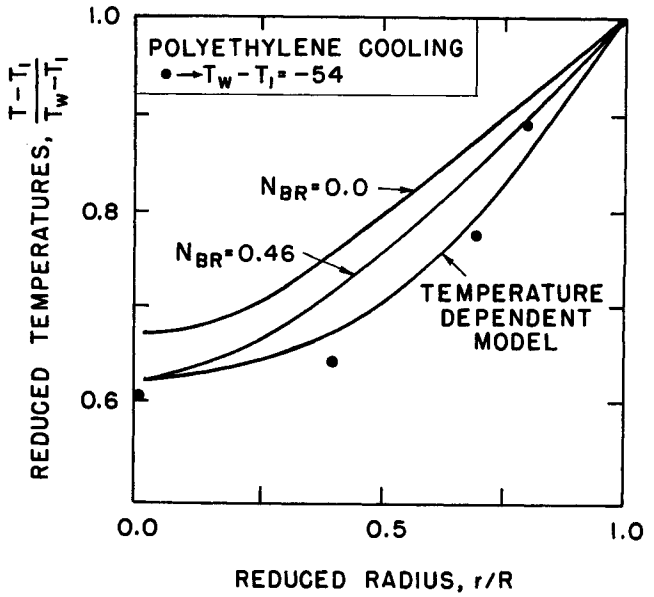


Fig. 3. Comparison of theoretical temperature profiles with experimental results for the cooling of polyethylene at a Graetz number of 7.74.

Figures 3 and 4 show that the temperature-dependent model more closely approximates the experimental data than either of the previous models for cooling of polyethylene. Figure 3 shows that at high flow rates, the viscous heating effect is greater (that is, temperatures are higher) than predicted by the previous studies. This is caused by the viscosity increase as the temperature-dependent fluid is cooled. In Figure 4, the temperature-dependent fluid model predicts a maxima in the temperature profile at low flow rates during cooling, as has been reported (*15*). This maxima results from a small viscous heat contribution to an otherwise flat temperature profile. At higher Graetz numbers the maxima is not observed because of conduction to the cooling liquid.

The temperature-dependent power-law rheological model does not greatly improve the accuracy of the calculated temperature profiles for heating or isothermal flow, over the simpler methods reported by Bird (*6*) and Toor (*8*), but substantial improvement is shown for cooling. This is because the previous fluid models could not predict increased viscosities due to cooling near the wall.

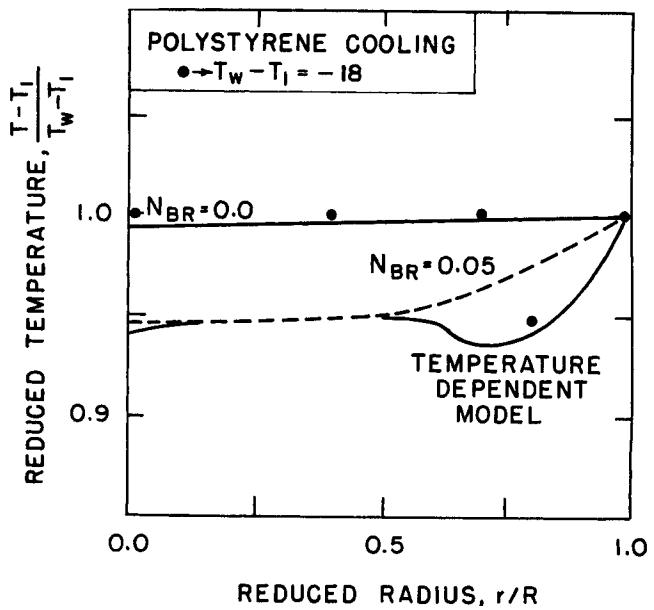


Fig. 4. Comparison of theoretical temperature profiles with experimental results for the cooling of polystyrene at a Graetz number of 2.33.

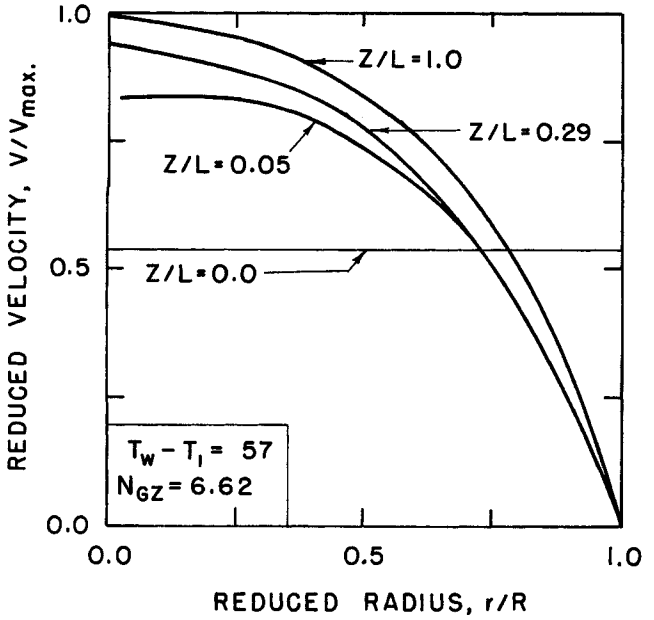


Fig. 5. Development of the velocity profile for heating of polyethylene.

The shape of the velocity profile is determined by the radial temperature profile and entrance length. Figures 5 and 6 compare the development of the velocity profiles for heating and cooling at several axial positions in the tube, as calculated from the temperature-dependent power-law fluid model. Because of the high Prandtl number, the velocity profile is transformed from flat to parabolic shortly after the polymer enters the tube. Near the tube exit ($z/L = 1.0$), expansion during heating causes an increase in fluid velocity. The velocity profile for cooling develops less uniformly than does the heating curve, probably because expansion of the polymer due to the decrease in pressure is opposed by contraction due to cooling.

The terminal velocity profile is a function of the radial temperature profile at the tube exit, and will be a function of flow rate only if the tube exit is in the entrance region. The heat exchanger used in this study was 3.7 ft. long, and entrance lengths were less than 26 in. (*15*). Hence, the terminal velocity profile was not a function of Graetz number. Figure 7 shows the terminal velocity profile for heating, cooling, and isothermal ($T_w \cong T_1$) flow of polyethylene obtained with the temperature-dependent model used in this study. Also shown is the theoretical velocity profile of an isothermal, incompressible, power-law fluid. Heating of the polymer causes lower viscosities near the wall, hence a flatter velocity profile. Cooling causes higher viscosities near the wall, and a less flat velocity profile results. At smaller Graetz numbers, the cooling and heating velocity profiles will converge toward the isothermal curve. The theoretical power-law and isothermal curves fall between the heating and cooling curves, but they do not coincide. This is due to cooling by expansion, which causes the isothermal curve for a compressible fluid to more closely approximate the cooling curve.

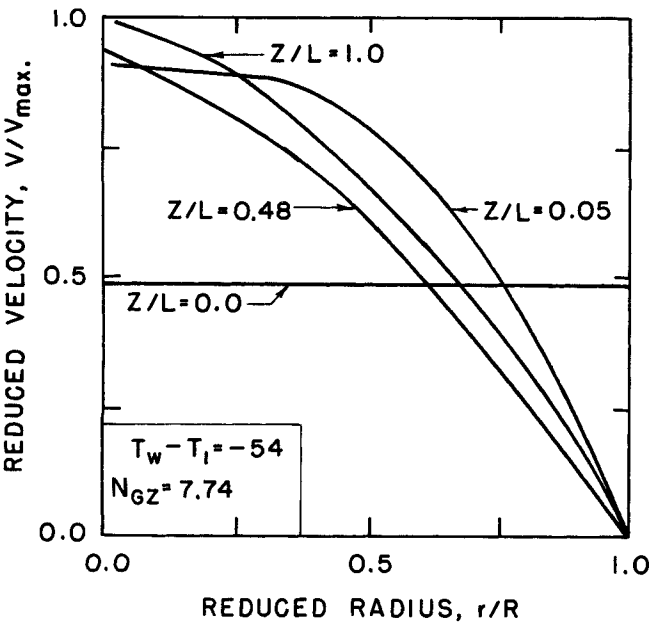


Fig. 6. Development of the velocity profile for cooling of polyethylene.

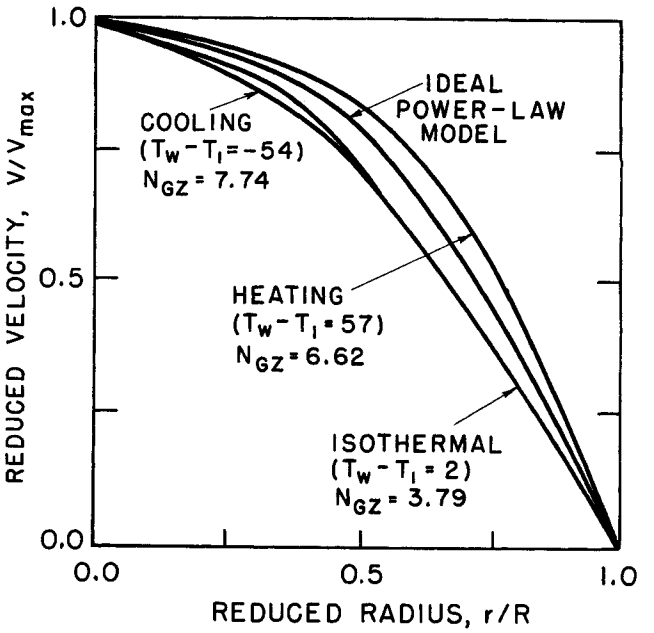


Fig. 7. Comparison of nonisothermal velocity profiles.

Figures 8 and 9 illustrate the development of the temperature profiles for heating and cooling. Each plot shows a gradual change from constant inlet temperature to a parabolic temperature profile. Changes in compressibility seem to have a larger effect on velocity profiles than they have on temperature profiles.

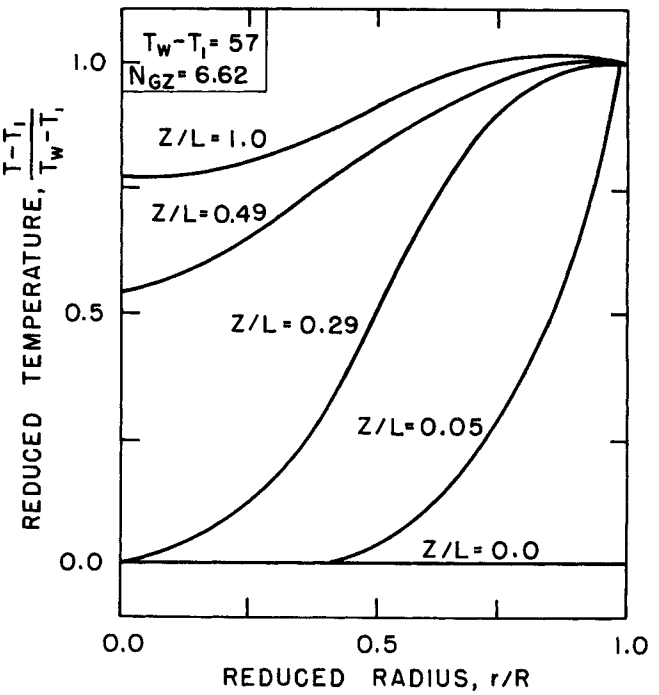


Fig. 8. Development of the temperature profile for the heating of polyethylene.

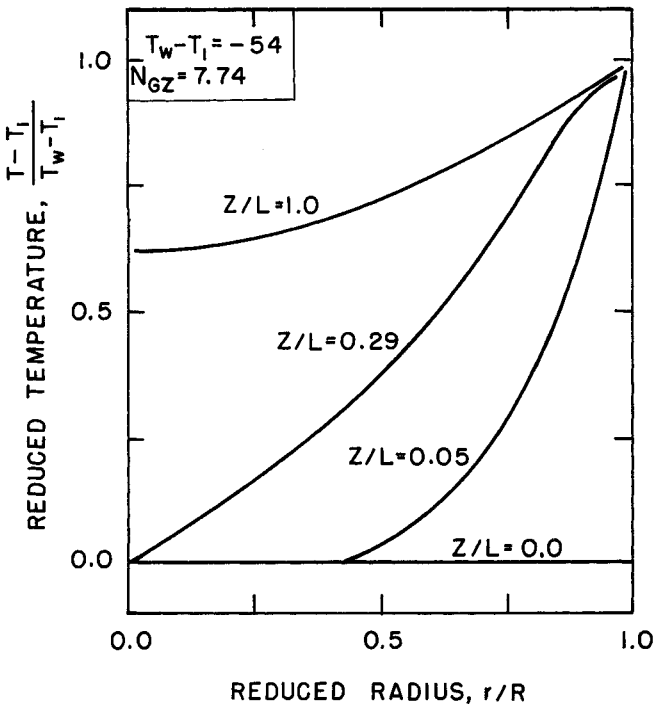


Fig. 9. Development of the temperature profile for the cooling of polyethylene.

## CONCLUSIONS

The conclusions of this study can be summarized as:

1. A generalized method for calculating temperature profiles of flowing power-law fluids during heating, cooling, and isothermal flow has been developed.
2. The temperature-dependent power-law rheological model with viscous heating effects is a more accurate method of predicting temperature profile calculations for cooling of polymer melts than previous models. Previous models are adequate for heating and isothermal flow of polymer melts.

## SUMMARY

Recent experimental studies have shown that existing methods of calculating the temperature profiles of molten flowing polymers are inadequate, particularly for polymer cooling.

The transport equations of continuity, momentum, and energy were solved by a digital computer for a compressible fluid with temperature-dependent power-law viscosity and temperature-dependent properties. The results obtained with this model are compared with previously reported results and previous theoretical results.

The results show that a compressible fluid model with temperature-dependent power-law viscosity and variable properties will predict the experimental results within 6%, which is a better prediction than obtained by previous theories. The experimentally observed maxima in the temperature profile for polymer cooling is due to increased heat generation because of the temperature-dependence of the power-law viscosity.

## NOTATION

$a$ = index number, Equation (19), dimensionless
$A$ = Arrhenius power-law constant, Equation (12), sec.$^n$ lb.$_f$/sq.ft.
$b$ = index number, Equation (19), dimensionless
$b_o$ = specific volume at absolute zero, cu.ft./lb.
$b_1$ = empirical constant, Equation (15), 1/°F.
$N_{Br}$ = modified Brinkman number, $\frac{Wr_w n}{\pi kR\,(3n+1)\,(T_w - T_1)}$, dimensionless
$c$ = empirical constant, Equation (16), 1/°F.
$C_p$ = heat capacity at constant pressure, B.t.u./lb.-°F.
$C_{po}$ = empirical constant, Equation (16), ft.-lb.$_f$/lb.-°F.
$C_v$ = heat capacity at constant volume, B.t.u./lb.-°F.
$N_{Gz}$ = Graetz number, $WC_p/kL$, dimensionless
$k$ = thermal conductivity, B.t.u./ft.-sec.-°F.
$k_o$ = empirical constant, Equation (15), ft.-lb.$_f$/sec.-ft.-°F.
$k_1$ = empirical constant, Equation (12), 1/°R.
$L$ = length of the heat exchanger, ft.
$M_w$ = molecular weight of a mer unit, lb./mole
$n$ = power law index, dimensionless
$P$ = pressure, lb.$_f$/sq.ft.
$P_o$ = arbitrary base pressure, lb.$_f$/sq.ft.
$r$ = radial distance from tube center, ft.
$R$ = inside radius of tube, ft.
$R_g$ = perfect gas law constant, 1.987 B.t.u./mole-°F.
$T$ = temperature at an arbitrary position, °F.
$T_o$ = arbitrary base temperature, °F.
$T_1$ = average polymer temperature at tube inlet, °F.
$T_r$ = reduced temperature, $T - T_1/T_w - T_1$, dimensionless
$T_w$ = temperature of the tube wall, °F.
$V_z$ = fluid velocity at an arbitrary position, parallel to tube axis, ft./sec.
$V_{\max}$ = maximum fluid velocity in the tube, ft./sec.
$W$ = mass flow rate, lb./sec.
$z$ = axial distance from tube inlet, ft.
$Z$ = value of a variable, Equation (19)

### Greek Letters

$\beta$ = compressibility, sq.ft./lb.$_f$
$\epsilon$ = thermal coefficient of expansion, °F.$^{-1}$
$\pi$ = internal pressure, Equation (13), lb.$_f$/sq.ft.
$\rho$ = density, lb./cu.ft.
$\rho_o$ = empirical constant, Equation (11), lb./cu.ft.
$\tau_{rz}$ = shear stress, lb.$_f$/sq.ft.
$\tau_w$ = shear stress at the wall, lb.$_f$/sq.ft.

## LITERATURE CITED

1. Metzner, A. B., R. D. Vaughan, and G. L. Houghton, *AIChE J.*, **3**, 92 (1957).
2. Chu, J. C., F. Brown, and K. G. Burridge, *Ind. Eng. Chem.*, **45**, 1686 (1953).
3. Christiansen, E. B., G. E. Jensen, and F. S. Tao, *AIChE J.*, **12**, 1196 (1966).
4. Pigford, R. L., *Chem. Eng. Progr. Symp. Ser. No. 17*, **51**, 79 (1955).
5. Topper, L., *Chem. Eng. Sci.*, **5**, 13 (1956).
6. Lyche, B. C., and R. B. Bird, *ibid.*, **6**, 35 (1956).
7. Bird, R. B., *Soc. Plastics Eng. J.*, **11**, 35 (1955).
8. Toor, H. L., *Ind. Eng. Chem.*, **48**, 922 (1956).
9. ———, *Trans. Soc. Rheol.*, **1**, 177 (1957).
10. ———, *AIChE J.*, **4**, 319 (1958).
11. Gee, R. E., and J. B. Lyon, *Ind. Eng. Chem.*, **49**, 956 (1957).
12. Beyer, C. E., and R. B. Dahl, *Mod. Plastics*, **30**, 124 (1964).
13. Schott, H., and W. S. Kaghan, *Soc. Plastics Eng. J.*, **20**, 139 (1964).
14. Griskey, R. G., and I. A. Wiehe, *AIChE J.*, **12**, 308 (1966).
15. Forsyth, T. H., Ph.D. thesis, Virginia Polytechnic Inst., Blacksburg (1967).
16. McKelvey, J. M., "Polymer Processing," p. 83, John Wiley, New York (1962).
17. Ibid., p. 41.
18. Ibid., p. 131.
19. Lapidus, L., "Digital Computation for Chemical Engineers," Chapt. 4, McGraw-Hill, New York (1962).
20. Brasie, W. C., *Chem. Eng. Progr.*, **58**, 48 (1962).

*Manuscript received February 2, 1968; revision received May 27, 1968; paper accepted May 31, 1968.*